International Journal of Heat and Mass Transfer 72 (2014) 139–147

Contents lists available at ScienceDirect

International Journal of Heat and Mass Transfer

journal homepage: www.elsevier.com/locate/ijhmt

Filter solution of inverse heat conduction problem using measured temperature history as remote boundary condition

Keith A. Woodbury [a,*], James V. Beck [b], Hamidreza Najafi [a]

[a] Mechanical Engineering Department, The University of Alabama, Tuscaloosa, AL 35487, USA
[b] Department of Mechanical Engineering, Michigan State University, East Lansing, MI 48824, USA

ARTICLE INFO

Article history:
Received 15 August 2013
Received in revised form 23 December 2013
Accepted 28 December 2013
Available online 29 January 2014

Keywords:
Inverse heat conduction
Filter solution
Temperature boundary condition

ABSTRACT

The inverse heat conduction problem (IHCP) involves estimation of a surface heat flux from transient temperature measurements inside a heat conducting body. Commonly an insulated remote boundary or one with a known heat transfer coefficient is modeled. However, in many practical applications, the precise thermal condition at the remote boundary is not known. In this paper, a method of accounting for thermal action at the remote boundary using a second measured temperature history is presented. The measurement need not be at an actual boundary but can be at an interior point in the domain.

The IHCP solution herein is achieved through the filter coefficient method, which uses filter coefficients in a convolution summation. By using the filter technique, near real-time heat flux measurements can be continuously obtained in manufacturing settings to enhance productivity. Also the filter concept opens the way for the development of new scientific instruments that incorporate inverse problem methods.

1. Introduction

The inverse heat conduction problem (IHCP) is typically defined as the problem of using internal temperature measurements to find heat fluxes on the surface. Sometimes this specific task is termed a *boundary IHCP* to emphasize recovery of the unknown surface heating action. The IHCP has been studied widely during last few decades, and notable texts have been authored by Beck et al. [1], Alifanov [2], Ozisik and Orlande [3] and Murio [4], to name a few. Several different methods have been developed and demonstrated for solving IHCPs. All boundary IHCP solutions assume full knowledge of the governing equation and thermal material properties, and full knowledge of boundary conditions on all but the active surface under investigation.

Remote boundaries are typically assumed to be insulated or cooled with a known heat transfer coefficient. For example, Ijaz et al. [5] consider estimation of heat flux histories on two faces of a two-dimensional domain. Their model assumes perfectly insulated surfaces on the other two faces, and temperature data are gathered on these insulated surfaces to drive the solution of the IHCP. Chen, et al. [6] also consider a two-dimensional problem, with two faces insulated, but the third face at a homogeneous temperature condition. In their method, the temperature, and not the heat flux, is determined on the fourth face of the domain. Mulcahy et al. [7] consider a problem in an annular three-dimensional geometry and seek the heat flux history on the inner surface of the annulus as a function of angle θ and axial coordinate z. They assume that all the other surfaces are insulated. Chan [8] performs an interesting study to determine the heat flux on a cylinder cooled by a jet. In this two-dimensional problem, measured temperatures on the surface of the cylinder are used to compute the heat flux on the cylinder, but this is done through solution of the flow field around the cylinder. In this case, insulated and no-slip boundaries are imposed on the bounding walls of the domain. Khajehpour et al. [9] tackle two-dimensional problems with finite element analysis and obtain solutions by splitting the domain into sub-regions. However, they do assume the remote boundaries are either insulated or have known convection cooling.

Chen, et al. [10] consider a slightly different problem. Their analysis of a one-dimensional domain considers two subsurface sensors, but seeks to compute the heat flux at both exposed surfaces.

Since IHCPs are mathematically ill-posed, an appropriate regularization method needs to be applied in order to convert the original ill-posed problem to a nearby well-posed problem and achieve a solution for it. Tikhonov regularization (TR) [11,12] is a common technique to stabilize the IHCP. It is commonly applied over the whole time domain which means that the solution procedure needs to access all the observations at once [1].

More recently, efforts have been made to develop real-time or filter forms for processing temperature data to solve the IHCP. Khorrami, et al. [13] employ an interesting approach based on the premise that the heat flux component at a particular time is

* Corresponding author. Tel.: +1 2053481647.
E-mail address: keith.woodbury@ua.edu (K.A. Woodbury).

0017-9310/$ - see front matter © 2014 Elsevier Ltd. All rights reserved.
http://dx.doi.org/10.1016/j.ijheatmasstransfer.2013.12.073

Nomenclature

C	volumetric specific heat, J/m^3-K
f	filter coefficients (X21 case)
$\mathbf{F}$	filter matrix (X21 case)
g	filter coefficients (X12 case)
G	Green's function
$\mathbf{G}$	filter matrix (X12 case)
k	thermal conductivity, W/m-K
L	location of temperature boundary condition, Eq. (3), m
m_f	number of future time steps
m_p	number of past time steps
q	heat flux, W/m^2
S	sum of squares of the temperature error, K^2
t	time, s
T	temperature, K
x	spatial coordinate, m
x'	dummy integration variable, Eq. (6)
$\mathbf{X}$	sensitivity matrix for unknown surface heat flux
y	measured temperature at boundary $x = L$
Y	measured temperature at location $x = x_1$
$\mathbf{Z}$	sensitivity matrix for measured temperature boundary condition at $x = L$

Greek/Roman

α	thermal diffusivity, k/C, m^2/s
α_T	Tikhonov regularization parameter
σ	standard deviation
σ_2	variance
β	eigenvalue
ϕ	step response function for unit heat flux at $x = 0$
η	step response function for unit temperature at $x = L$
τ	integration variable, Eq. (6)

Subscripts

0	surface location or reference value
1	location of measurement sensor
i	time index
m	eigenvalue index
M	time index; any time, or the current time
ss	steady state
N	last time index
X21	Cartesian heat conduction problem with type 2 and type 1 boundary conditions

Superscript

$\sim$	dimensionless parameter

a linear combination of the temperature around the time of its occurrence. They use an artificial neural network to determine the required coefficients of the linear filter based on detailed numerical simulation of the target process. Deng and Hwang [14] also use artificial neural networks to generate the filter solutions for heat flux estimation based on temperature histories. Ijaz et al. [5] solve a transient IHCP by using Kalman filter. LeBreux et al. [15] use a combination of Kalman filtering and recursive least squares to achieve a real-time algorithm to determine heat flux history for industrial applications. Lamm [16,17] employs a sequential computation based on TR by using a recent subset of available data and a limited number of past predictions and observations. Cabeza, et al. [18] studied the filter effect of the function specification method and the truncated singular value decomposition method in a sequential form [19]. By examining the power spectral densities of the two methods, they concluded that the regularization methods act as band-pass filters. Most recently, Woodbury and Beck [20] study the structure of the TR problem and conclude that the method can be interpreted as a sequential filter formulation for continuous processing of data. They show that the computed heat fluxes using the whole domain solution and the filter coefficient solution are virtually the same for the constant-property solutions.

The filter method [1,20] used in this paper is a representation of one of many IHCP solution methods, such as Tikhonov Regularization, in a digital filter form. It is not a new or different method of solving IHCPs, but merely a representation of the solution in a form suitable for continuous (online) processing of data.

Measuring heat flux has great significance in several scientific experiments as well as industrial applications such as monitoring manufacturing processes and fire safety tests. Digital filter solutions are especially advantageous for developing new instruments for near real-time heat flux estimation from continuous temperature histories.

In this paper, a method is developed to incorporate the temperature measurement history from a second subsurface sensor as a remote boundary condition in an IHCP solution. The second measurement may, or may not, coincide with the physical boundary of the domain. Tikhonov regularization is used to stabilize the solution and the resulting algorithm is written in filter form [20]. An example problem is considered and both the whole domain method and the sequential filter solution method are illustrated. The filter solution of the IHCP has a number of advantages including simplicity, continuous operation and application to moderate nonlinearity manifested by temperature-dependent thermal properties [21] which makes it an appropriate approach for near real-time heat flux estimation.

2. Problem description

The IHCP solution typically starts by minimizing a sum of squares function, which is the sum of the squares of the difference between the measured and calculated temperatures at a location x_1. The calculated temperatures are functions of the unknown surface heat flux. Some form of regularization is needed, and the function specification method [1] or Tikhonov regularization (TR) [11,12] are only two of many techniques. For the function specification method, the heat flux is found using a sum of squares function that uses both past and future information. The Tikhonov whole domain regularization method will have a sum of squares function over the total time domain. However, the nature of the IHCP is such that a given heat flux component is a linear function of only a limited number of past and future measured temperatures. This point is illustrated below.

For simplicity, at this point a sum of squares function over the total time domain will be used in this analysis. Furthermore this time domain is large enough so that there is a long middle time region in which the very early conditions and the final time conditions have negligible effect upon the heat flux. This, too, is discussed further below.

The describing heat conduction equation is

$$\frac{\partial}{\partial x}\left(k\frac{\partial T}{\partial x}\right) = C\frac{\partial T}{\partial t}, \quad 0 < x < L, \; t > 0 \tag{1}$$

This equation permits the thermal conductivity, k, and the volumetric heat capacity, C, to be functions of temperature. However, in the derivation that follows, these properties are considered constants. It is found that the filter solution of the nonlinear IHCP for moderate changes in the properties is sufficiently accurate [21]. In this case, the filter coefficients need to be found for different temperatures using corresponding material properties and then by applying linear interpolation the values of filter coefficients can be found for each time step. Eq. (1) implies that the problem is one-dimensional Cartesian, side heat losses are not present and no internal heat sources are present. A consequence of all these observations is that it usually is not necessary to attempt to estimate the heat flux extremely accurately, such as to one or two percent of the maximum value. With no loss of generality, the initial temperature is considered to be zero,

$$T(x,0) = 0 \tag{2}$$

Fig. 1 illustrates the one-dimensional domain and summarizes the nomenclature. The temperature history at a location $x = L$ is measured and is used as a boundary condition. This measurement location may be at a physical boundary, or may be at a subsurface location within the domain. Hence, the plate can be much thicker than the length L and heat may be flowing though the plane at L. The measured temperature boundary condition is expressed as

$$T(L,t) = y(t) \tag{3}$$

The temperature is also measured at a point x_1, where $0 \le x_1 < L$. This data serves as supplemental data required for solution of the IHCP. This measured data is written as

$$\hat{T}(x_1,t) = Y(t) \tag{4}$$

where $\hat{T}$ indicates an estimate of the temperature at x_1. It is an estimate since it is a measured value which has some errors. The location x_1 is between zero and L but, in practice, x_1 should be equal to or smaller than $L/2$, smaller being better.

The objective of the IHCP is to estimate the surface heat flux,

$$-k\frac{\partial T}{\partial x}(0,t) = q(t) = ? \tag{5}$$

using information coming from the measured temperatures indicated by Eq. (4). A sum of squares function over the complete time domain is

$$S = \sum_{i=1}^{N}(Y_i - T(x_1,t_i))^2 \tag{6}$$

where $T(x_1, t_i)$ is calculated and is a function of the unknown heat flux components. An expression is needed for this term. This

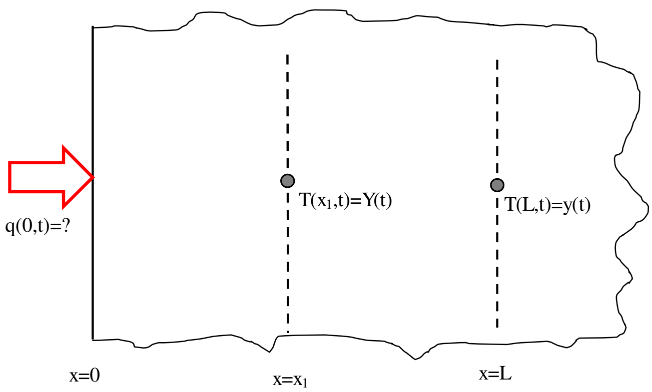

Fig. 1. Physical domain and nomenclature. Note location L may, or may not, coincide with the location of a physical boundary, and location x_1 can be in the range $0 \le x_1 \le L$.

temperature is a function of the heat flux and the given temperature at $x = L$. These temperatures can be computed using a numerical method, such as Crank-Nicolson, or using an exact solution, which is used in this paper, but either one can be used. When using Tikhonov regularization another term is added to the sum of squares, such as the sum of squares of the heat flux components.

3. Temperature computation using an exact procedure

The temperature at x_1 is a function of the surface heat flux $q(t)$ and the temperature at $x = L$. One exact way to obtain the temperature uses Green's functions [22]; an expression is

$$T(x_1,t) = \frac{\alpha}{k}\int_{\tau=0}^{t} q(\tau)G_{X21}(x_1,0,t-\tau)\,d\tau + \alpha\int_{\tau=0}^{t} y(\tau)\left(-\frac{\partial G_{X21}}{\partial x'}(x_1,L,t-\tau)\right)d\tau \tag{7}$$

The Green's function in this equation is for a boundary condition of the second kind (a gradient condition, also called Neumann) at $x = 0$ and the first kind (specified temperature, also called Dirichlet) at $x = L$. The notation X21 denotes a Cartesian geometry with a boundary condition of the second kind at $x = 0$ and the first kind at $x = L$. In using Eq. (7) with equally spaced times, it is necessary to specify the type of variation between adjacent times. At this point, the heat flux components, q_i and q_{i+1}, and also between adjacent temperature components, y_i and y_{i+1}, are specified as being constant between time points (step function); but they could also be linear, quadratic and cubic. The step variation can be described by

$$q(t) = q_i, \quad t_i < t < t_{i+1} \tag{8a}$$

$$t_i = i\Delta t \tag{8b}$$

A solution for the X21 case with a constant heat flux at $x = 0$ and zero temperature at $x = L$ is [23]

$$\frac{T(x,t)}{q_0L/k} = \left(1-\frac{x}{L}\right) - 2\sum_{m=1}^{\infty} e^{-\beta_m^2\frac{\alpha t}{L^2}}\frac{\cos(\beta_m\frac{x}{L})}{\beta_m^2} \tag{9}$$

where $\beta_m = (m - 1/2)\pi$, $m = 1, 2, \ldots$ (The notation used to describe these solutions is sometimes referred to the BCHL notation, after the authors of Ref. [22]. The BCHL notation for this case is X21B10T0. More information on the notation can be found in Refs. [22] and [24].) For a constant (step) heat flux input, the dimensionless temperatures at $x = x_1$ for times $t = \Delta t, 2\Delta t, \ldots, i\Delta t$ are designated $\phi_1, \phi_2, \ldots, \phi_i$. These values are termed the *response function* and represent the dimensionless temperature rise at the measurement location due to a unit disturbance (step change) in the surface condition. More explicitly the ith value, ϕ_i, is

$$\phi_i = \frac{T(x_1,i\Delta t)}{q_0L/k} = \left(1-\frac{x_1}{L}\right) - 2\sum_{m=1}^{\infty} e^{-\beta_m^2\frac{\alpha i\Delta t}{L^2}}\frac{\cos\left(\beta_m\frac{x_1}{L}\right)}{\beta_m^2} \tag{10}$$

Likewise, in consideration of a step change in temperature at the boundary $x = L$, the solution for a constant temperature, T_0, at $x = L$ is

$$\frac{T(x,t)}{T_0} = 1 - 2\sum_{m=1}^{\infty} e^{-\beta_m^2\frac{\alpha t}{L^2}}\frac{\sin\left(\beta_m(1-\frac{x}{L})\right)}{\beta_m} \tag{11}$$

and the eigenvalues are the same as given below Eq. (9) (the BCHL notation for this case is X21B01T0). Analogous to ϕ_i, the response function at x_1 for a constant temperature disturbance T_0 at $x = L$, denoted as η_i, is

$$\eta_i = \frac{T(x_1,i\Delta t)}{T_0} = 1 - 2\sum_{m=1}^{\infty} e^{-\beta_m^2\frac{\alpha i\Delta t}{L^2}}\frac{\sin\left(\beta_m(1-\frac{x_1}{L})\right)}{\beta_m} \tag{12}$$

Using Eqs. (10) and (12), the temperature at x_1 can be found for any time-variable heat flux at $x = 0$ and temperature variation at $x = L$

through scaling and superposition of the response functions. If the heat flux is piecewise constant, and the temperature variation at $x = L$ is piecewise constant, the result from the following procedure is exact. Since Eq. (7) indicates the $q(t)$ and $y(t)$ inputs can be added (because of linearity), the two components of Eq. (7) can be considered separately. First, consider the temperature response at x_1 due to a piecewise constant heat flux at $x = 0$. Using step (piecewise-constant) basis functions with an initial temperature equal to zero, the temperatures at t_i, $i = 1, 2, \ldots, M$ are found by scaling the unit responses and superposition and can be written as

$$\begin{aligned}
T_{q,1} &= T_q(x_1, \Delta t) = \frac{L}{k}(q_1 \Delta\phi_0) \\
T_{q,2} &= T_q(x_1, 2\Delta t) = \frac{L}{k}(q_1 \Delta\phi_1 + q_2 \Delta\phi_0) \\
&\vdots \\
T_{q,M} &= T_q(x_1, M\Delta t) = \frac{L}{k}\sum_{i=1}^{M} q_i \Delta\phi_{M-i}
\end{aligned} \tag{13a}$$

which can be written as

$$\begin{aligned}
T_{q,1} &= q_1 X_1 \\
T_{q,2} &= q_1 X_2 + q_2 X_1 \\
&\vdots \\
T_{q,M} &= q_1 X_M + q_2 X_{M-1} + \cdots + q_{M-1} X_2 + q_M X_1 = \sum_{i=1}^{M} q_i X_{M-i+1}
\end{aligned} \tag{13b}$$

where, in Eq. (13a),

$$\Delta\phi_i = \phi_{i+1} - \phi_i \tag{14}$$

Note that, in Eq. (14), $\phi_0 = 0$, so that $\Delta\phi_0 = \phi_1$. In Eq. (13a) and (13b), the q subscript on T denotes that it is the contribution to the temperature at x_1 caused by the unknown heat flux.

Similarly the contribution to the temperature at x_1 due to the temperature history at $x = L$ is

$$T_{y,M} = \sum_{i=1}^{M} y_i \Delta\eta_{M-i} \tag{15a}$$

which can be written as

$$T_{y,M} = \sum_{i=1}^{M} y_i Z_{M-i+1} \tag{15b}$$

Then the temperature at x_1 caused by the heat flux at $x = 0$ and the temperature at $x = L$ is the sum of the two contributions:

$$\begin{aligned}
T_M = T_{q,M} + T_{y,M} &= \frac{L}{k}\sum_{i=1}^{M} q_i \Delta\phi_{M-i} + \sum_{i=1}^{M} y_i \Delta\eta_{M-i} \\
&= \sum_{i=1}^{M} q_i X_{M-i+1} + \sum_{i=1}^{M} y_i Z_{M-i+1}
\end{aligned} \tag{16}$$

The step basis function representations (and also for other basis functions) for temperature given in Eq. (16) can be described by the matrix equation of

$$\mathbf{T} = \mathbf{Xq} + \mathbf{Zy} \tag{17}$$

where

$$\mathbf{T} = \begin{bmatrix} T_1 \\ T_2 \\ \vdots \\ T_n \end{bmatrix}, \quad \mathbf{q} = \begin{bmatrix} q_1 \\ q_2 \\ \vdots \\ q_n \end{bmatrix}, \quad \mathbf{X} = \begin{bmatrix} X_1 & 0 & 0 & \cdots & 0 & 0 \\ X_2 & X_1 & 0 & \cdots & 0 & 0 \\ X_3 & X_2 & X_1 & \cdots & 0 & 0 \\ \vdots & \vdots & \vdots & & \vdots & \vdots \\ X_n & X_{n-1} & X_{n-2} & \cdots & X_2 & X_1 \end{bmatrix} \tag{18a, b, c}$$

$$\mathrm{y} = \begin{bmatrix} y_1 \\ y_2 \\ \vdots \\ y_n \end{bmatrix}, \quad \mathrm{Z} = \begin{bmatrix} Z_1 & 0 & 0 & \cdots & 0 & 0 \\ Z_2 & Z_1 & 0 & \cdots & 0 & 0 \\ Z_3 & Z_2 & Z_1 & \cdots & 0 & 0 \\ \vdots & \vdots & \vdots & & \vdots & \vdots \\ Z_n & Z_{n-1} & Z_{n-2} & \cdots & Z_2 & Z_1 \end{bmatrix} \tag{19a, b}$$

The components of the **X** and **Z** matrices are related to the characteristic response functions by

$$X_i = \frac{L}{k}\Delta\phi_{i-1}, \quad Z_i = \Delta\eta_{i-1} \tag{20a, b}$$

The units of **X** are temperature per unit heat flux; those for **Z** are temperature per unit temperature (dimensionless). The columns in the **X** matrix of Eq. (18) are the same as the sensitivity vectors in parameter estimation. The first column is for q_1, the second for q_2 and so on. Notice that these sensitivity coefficient vectors are the same as each successive column of values is simply shifted down by one. Although there might be hundreds of heat flux components, their basic characteristics can be inferred from just examining the first column (the sensitivity vector). The effect of estimating multiple components can be inferred by shifting this curve (or vector) one unit.

When the columns of the **X** matrix are identified as comprised of the sensitivity components, related important concepts of parameter estimation can be introduced. Two concepts are that the sensitivity vectors should 1) be large in magnitude and 2) be uncorrelated. (Actually, the scaled sensitivities are examined in which each sensitivity, $\circ T_i/\circ q_1$, is multiplied by q_1. This provides the same units of temperature so the sensitivities can be compared with each other and with the magnitude of the temperature rise itself.) These aspects of magnitude and uncorrelated sensitivity coefficients are examined below.

In light of the above comments, the scaled sensitivity coefficients for the heat flux components are examined. Note from Eq. (20a) that the X_i's are the differences between successive values of the $\phi(i\Delta t)$ curve in Eq. (10) for a particular value of Δt multiplied by the ratio L/k. Algebraic expressions for the scaled sensitivity coefficients can be found using Eqs. (10) and (20a). The first one is given by:

$$\begin{aligned}
q_1 \frac{\partial T(x_1, \Delta t)}{\partial q_1} &= q_1 X_1 = q_1 \Delta\phi_0 = q_1 \phi_1 \\
&= \frac{q_1 L}{k}\left\{\left(1 - \frac{x_1}{L}\right) - 2\sum_{m=1}^{\infty} e^{-\beta_m^2 \frac{\alpha \Delta t}{L^2}} \frac{\cos\left(\beta_m \frac{x_1}{L}\right)}{\beta_m^2}\right\}
\end{aligned} \tag{21a}$$

All the other scaled sensitivity coefficients can be found as

$$\begin{aligned}
q_1 \frac{\partial T(x_1, i\Delta t)}{\partial q_1} &= q_1 X_i = q_1 \frac{L}{k}\Delta\phi_i = q_1 \frac{L}{k}(\phi_i - \phi_{i-1}) \\
&= \frac{q_1 L}{k}\left\{2\sum_{m=1}^{\infty}\left(e^{-\beta_m^2 \frac{\alpha(i-1)\Delta t}{L^2}} - e^{-\beta_m^2 \frac{\alpha i \Delta t}{L^2}}\right) \frac{\cos\left(\beta_m \frac{x_1}{L}\right)}{\beta_m^2}\right\}
\end{aligned} \tag{21b}$$

where

$$X_i = \frac{\partial T(x_1, i\Delta t)}{\partial q_1} \tag{21c}$$

Eqs. (21a,b) show that the sensitivity coefficients are functions of the sensor location, x_1, and the time step in the data, Δt. The behavior of these coefficients as functions of these two variables is investigated.

The scaled sensitivity coefficients are illustrated in Fig. 2 and Fig. 3. For convenience, dimensionless forms of the equations are treated by plotting

$$\frac{q_1 X_i}{q_1 L/k} = \tilde{X}_i \tag{22}$$

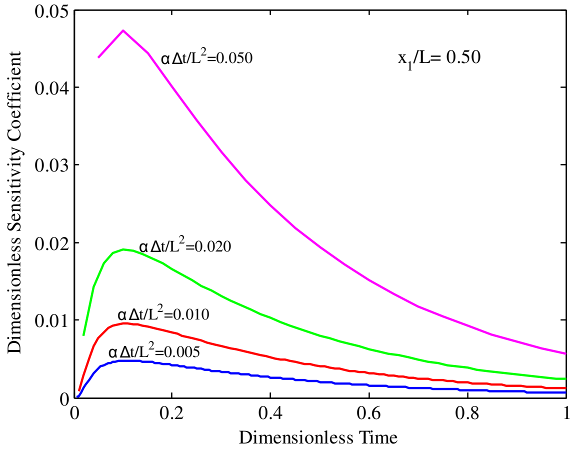

Fig. 2. Components of the dimensionless sensitivity vector X for the heat flux at $x = 0$ for sensor at $x_1/L = 0.5$ for different time steps $\alpha\Delta t/L^2$. (Plot_X.m).

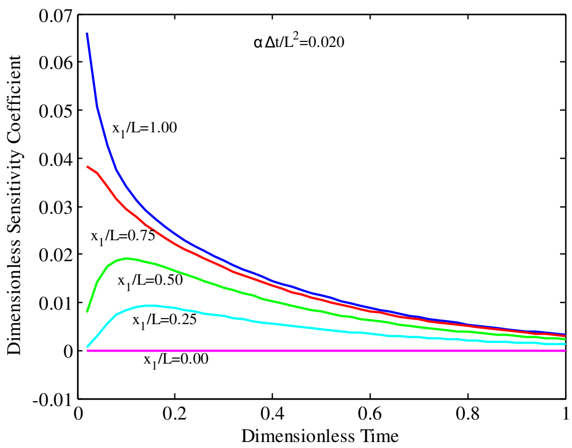

Fig. 3. Components of the sensitivity vector X for the heat flux at $x = 0$ for time step $\alpha\Delta t/L^2 = 0.02$ and various sensor locations $x_1/L = 0.0$, 0.25, 0.50, 0.75, 1.0. (Plot_X2.m).

versus dimensionless time. Fig. 2 shows the components of X for a sensor located at $x_1/L = 0.5$ for different values of dimensionless time step $\alpha\Delta t/L^2$. Fig. 2 indicates that higher values of dimensionless time step result in higher sensitivity coefficients. From a parameter estimation point of view, this is highly desirable. However, the time step in the data also controls the resolution of the heat flux history, and larger time steps will only permit coarser piecewise constant representations of the heat flux. A balance between increased sensitivity and fidelity of the heat flux function must be struck.

Fig. 3 shows the components of the sensitivity vector X for a fixed time step of $\alpha\Delta t/L^2 = 0.02$ for sensor locations at $x_1/L = 0.0$, 0.25, 0.5, 0.75, and 1.0. The highest sensitivities result from sensor locations closest to the heated surface, and zero sensitivity results from sensors at $x_1 = L$.

The procedure above outlines an approach for linear problems, in particular a heat conduction problem when the thermal properties of the material are invariant. However, it has been demonstrated [21] that this approach can be extended to the moderately non-linear case of temperature-dependent thermal properties by computing digital filter coefficients corresponding to properties at different discrete temperature levels and interpolating between them based on the level of temperature at the present time.

4. IHCP solution using Tikhonov regularization

The whole domain Tikhonov regularization method [1,25] is used to solve the IHCP. Later the filter coefficients are found from the solution. The solution starts with a matrix form for the sum of squares with an added regularization term given by

$$S = (\mathbf{Y} - \mathbf{Xq} - \mathbf{Zy})^T(\mathbf{Y} - \mathbf{Xq} - \mathbf{Zy}) + \alpha_T\mathbf{q}^T\mathbf{H}^T\mathbf{Hq} \tag{23}$$

S is minimized with respect to the parameter vector $\mathbf{q}$. The symbol $\mathbf{Y}$ is the temperature measurement vector at x_1 and $\mathbf{y}$ is the measured boundary temperature at $x = L$. The initial temperature is zero. The α_T symbol is the Tikhonov regularization parameter which controls the degree of regularization (and bias!) introduced into the solution. Various orders of regularization can be selected and are implemented via the matrix $\mathbf{H}$. The first order method is selected here which uses first differences of the heat flux components. The matrix operator $\mathbf{H}$ is a forward difference approximation for the first derivative of $\mathbf{q}$ (see [1, page 139].) The estimated value heat flux vector, denoted $\hat{\mathbf{q}}$, is found by minimizing S with respect to $\mathbf{q}$ and is given by

$$\hat{\mathbf{q}} = [\mathbf{X}^T\mathbf{X} + \alpha_T\mathbf{H}^T\mathbf{H}]^{-1}\mathbf{X}^T(\mathbf{Y} - \mathbf{Zy}) = \mathbf{F}(\mathbf{Y} - \mathbf{Zy}) = \mathbf{FY} + \mathbf{Gy} \tag{24}$$

Note that this equation is dimensional. $\mathbf{F}$ has the same definition as the filter matrix of Ref. [20], however in the present application it is defined with the $\mathbf{X}$ matrix from the X21B10T0 case and Ref. [20]considers the X22B10T0 case. The units of $\mathbf{F}$ are heat flux per unit temperature (W/m^2-K). In Eq. (24), the term $\mathbf{Zy}$ can be viewed as a modification or "correction" to the measured data $\mathbf{Y}$ to account for the contribution of the non-homogeneous boundary condition at $x = L$ to the measured Y_i values. Recall that, although Eq. (24) is dimensional, the matrix $\mathbf{Z}$ is dimensionless.Finally, observe that this equation is a linear function of the measurement temperature vectors $\mathbf{Y}$ and $\mathbf{y}$. This is important for the filter method of analysis of the IHCP.

5. Filter algorithm

The concept of the IHCP filter is described in Ref. [1], but explained in more detail in Ref. [20]. It should be noted that the filter "solution" is really a representation of a particular IHCP solution, such as Tikhonov regularization or future time step method, in a digital filter. This is possible because the solution for the heat flux at any time is only affected locally by the recent temperature history and a limited number of future time steps. This facilitates "near real-time" computation of heat fluxes based on temperature measurements just prior and just slightly ahead of the "present" time. Temperature measurements in the distant past and far future do not have significant impact of the physics of the present. Efficient, rapid computation of the heat flux very near the "present" time makes this formulation suitable for implementation in a microprocessor-based instrument for measuring heat fluxes in a continuous process.

Consider for the moment only the portion of the temperature disturbance at x_1 due to the heat flux at $x = 0$. The portion of the heat flux due to the measured temperature at x_1 for a particular time, t_M, can be computed as

$$\begin{aligned}\hat{q}_{M,Y} &= f_1Y_{M+m_f} + f_2Y_{M+m_f-1} + \cdots + f_{m_f}Y_M + \cdots + f_{M+m_p-1}Y_{M-m_p+1} \\ &\quad + f_{M+m_p}Y_{M-m_p} = \sum_{i=1}^{m_p+m_f} f_iY_{M+m_f-i}\end{aligned} \tag{25}$$

where the f's are elements of a *filter vector*, and m_f refers to the number of future times steps, and m_p refers to the number of past time steps. The elements of this vector are the non-zero entries of a column of the $\mathbf{F}$ matrix in Eq. (24). The $\mathbf{F}$ matrix for the

X22B10T0 case (denoted $\mathbf{F}_{X22}$) and its properties are described in detail in Ref. 20. The **F** matrix for the X21B10T0 case (denoted $\mathbf{F}_{X21}$) has many similar properties, notably that, except for the first few and last few rows, the entries on each row are identical but shifted in time by one time step.

The entries of the middle column of the $\mathbf{F}_{X21}$ matrix are plotted in Fig. 4 for different sensor locations x_1/L. It is seen that the width or range of the filter, determined by the interval with non-zero values, increases as the sensor depth increases. This indicates that the number of time steps of data required for resolving the surface heat flux increases with distance of the sensor from the active surface. This is related to the fact that the magnitudes of the entries of the sensitivity matrix **X** decrease with distance from the surface. Sensor locations closer to the surface will have higher sensitivity to the unknown heat flux and will result in a digital filter with the smallest width.

As indicated by Eq. (24), an additional term is needed beyond Eq. (25) to account for the changing temperature at $x = L$. This term, $\mathbf{Gy} = -\mathbf{FZy}$, can also be written in a filter form as

$$\hat{q}_{M,y} = g_1 y_{M+m_f} + g_2 y_{M+m_f-1} + \cdots + g_{m_f} y_M + \cdots + g_{M+m_p-1} y_{M-m_p+1} + g_{M+m_p} y_{M-m_p} = \sum_{i=1}^{m_p+m_f} g_i y_{M+m_f-i} \tag{26}$$

where $\hat{q}_{M,y}$ is the estimate for the portion of the heat flux at $x = 0$ due to the measured temperature at $x = L$. Many of the properties of the filter matrix **G** are similar to those of the matrix **F**, in particular that the rows of the matrix, except for the first few and last few, have all the same values, but each row is shifted over by one time step. Likewise, all the columns are the same, but each successive one shifted down by one row. Also, the values on each row and column vanish to zero for small and large times.

Fig. 5 illustrates the middle column of the **G** matrix for different sensor depths. The values plotted are the entries of the **g** vector. The width or range of the **g** filter is determined by the number of non-zero entries. It is seen in Fig. 5 that the width of the filter increases with smaller sensor depths. This peculiarity can be understood since the measured temperature is at the remote boundary ($x = L$), and sensor locations further from this active boundary are at smaller values of x. Fig. 5 also indicates that the values of **g** are predominantly negative.

The complete estimator for the surface heat flux at time t_M is found as the sum of Eq. (25) and (26) as follows

$$\begin{aligned} \hat{q}_M = & \sum_{i=1}^{m_f+m_p} (f_i Y_{M+m_f-i} + g_i y_{M+m_f-i}) \\ = & f_1 Y_{M+m_f-1} + f_2 Y_{M+m_f-2} + \cdots + f_{m_f-1} Y_{M+1} + f_{m_f} Y_M \\ & + f_{m_f+1} Y_{M-1} + \cdots + f_{m_p+m_f} Y_{M-m_p} + g_1 y_{M+m_f-1} \\ & + g_2 y_{M+m_f-2} + \cdots + g_{m_f} y_M + g_{m_f+1} y_{M-1} + \cdots \\ & + g_{m_p+m_f} y_{M-m_p} \end{aligned} \tag{27}$$

Note that all the f-filter coefficients can be found at one time by setting all the **Y** and **y** components equal to zero except the m_f component, Y_{m_f}, in Eq. (27) is set equal to one. To get the g-filter coefficients (those for the **y** vector), the same procedure is followed with now all the components of **Y** and **y** equal to zero except $y_{m_f} = 1$.

Figs. 6 and 7 depict the **f** and **g** filter coefficients for the location $x_1/L = 0.5$; the first order Tikhonov parameter value of α_T is equal to 0.0001 in Fig. 6 and 0.01 in Fig. 7. In both cases the filter coefficients for **f** is the largest, by about a factor of 10 in Fig. 6 and a factor of 4 in Fig. 7. Having **f** larger than **g** indicates that errors in the temperature boundary condition at $x = L$ are less significant than those at x_1. Also note that the range of non-zero values in Fig. 6

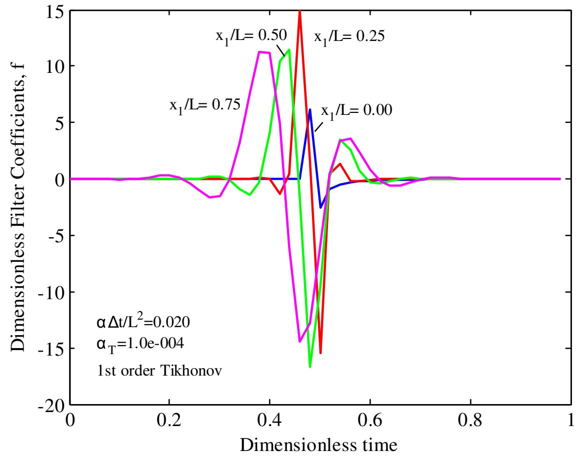

Fig. 4. Dimensionless filter coefficients f for the surface heat flux at $x = 0$ for various sensor locations x_1/L. First order Tikhonov regularization $\alpha_T = 1\text{e}{-4}$. $m_f = m_p = 25$. (compute_F_X21.m).

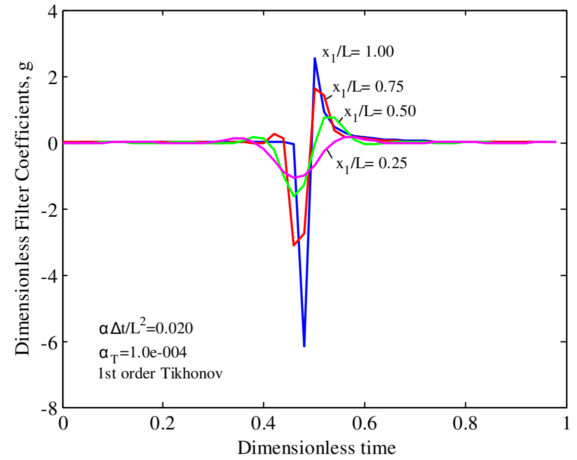

Fig. 5. Dimensionless filter coefficients g for the measured temperature at $x = L$ for various sensor locations x_1/L. First order Tikhonov regularization $\alpha_T = 1\text{e}{-4}$. $m_f = m_p = 25$. (compute_G_X21.m).

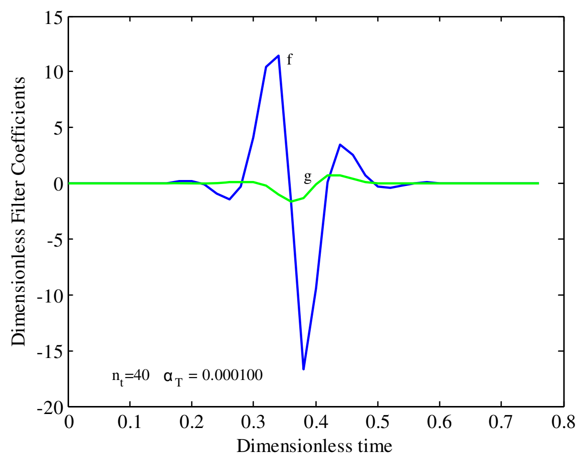

Fig. 6. Filter coefficients f for $Y(20) = 1$ and others zero and g for $y(20) = 1$ and others zero. $m_p = 20$ and $m_f = 20$. $\alpha\Delta t/L^2 = 0.02$. $\alpha_T = 0.0001$. $\Sigma f = 2.002144$, $\Sigma g = -1.999706$. Range of non-zero values about $0.15 < \alpha t/L^2 < 0.6$. (compute_fg_X21_2.m).

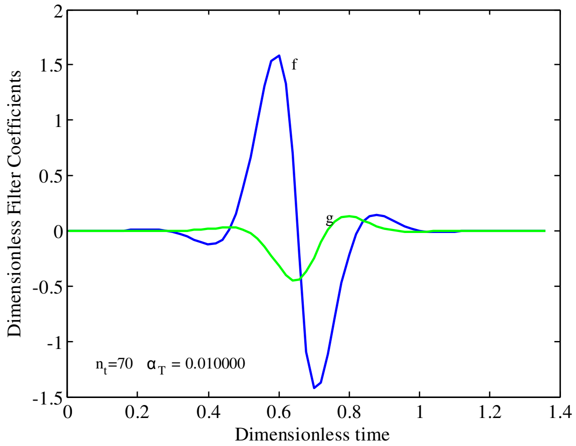

Fig. 7. Filter coefficients f for $Y(34) = 1$ and others zero and g for $y(34) = 1$ and others zero. $m_p = 35$ and $m_f = 35$. $\alpha\Delta t/L^2 = 0.02$. $\alpha_T = 0.01$. $\Sigma f = 2.002937$, $\Sigma g = -1.999715$. Range of non-zero values about $0.3 < \alpha t/L^2 < 1.1$. (compute_fg_X21_2.m).

is about $0.15 < \alpha t/L^2 < 0.6$ or spans about 0.45 in dimensionless time. The corresponding range in Fig. 7 is from $0.3 < \alpha t/L^2 < 1.1$ or spans about 0.8. Hence more regularization (i.e., larger α_T), increases the range of the filter coefficients. Also, as α_T is increased, the magnitude of the filter coefficients decreases. The magnitudes are important. For example, suppose that the heat flux is being estimated and there is a single error of 1 in the temperature at a given time. This would cause an error in the estimated heat flux for $\alpha_T = 0.0001$ that briefly reaches 15 (the magnitude of f in Fig. 6) and only about one-tenth of that for $\alpha_T = 0.01$, as shown by Fig. 7.

The maximum value of the absolute values of the filter coefficients increases as the Tikhonov parameter decreases. However, the sum of the **f** filter coefficients is a constant for a given location x_1. This concept was explored in Ref. [20] for the X22 case and is described here for the X21 case. Information regarding the sums of the coefficients in Fig. 6 or Fig. 7 can be obtained by using the filter equation given by Eq. (27); this equation can be used for transient and steady state situations. Let it now be used for steady state and many measurements in time. These temperatures are constants which are here denoted by Y_{ss} and y_{ss}. Then Eq. (27) can be used to obtain

$$\hat{q}_M = \hat{q}_{ss} = \sum_{i=1}^{m_p+m_f} (f_i Y_{M+m_f-i} + g_i y_{M+m_f-i}) = \sum_{i=1}^{m_p+m_f} (f_i Y_{ss} + g_i y_{ss}) \\ = Y_{ss} \sum_{i=1}^{m_p+m_f} f_i + y_{ss} \sum_{i=1}^{m_p+m_f} g_i \tag{28}$$

For steady-state heat conduction in a plate with fixed temperatures at x and L, the heat flux is given by

$$q_{ss} = -k\frac{\Delta T}{\Delta x} = -k\frac{y_{ss} - Y_{ss}}{L - x} = k\frac{Y_{ss}}{L - x} - k\frac{y_{ss}}{L - x} \tag{29}$$

Equating the above two equations gives

$$Y_{ss} \sum_{i=1}^{m_p+m_f} f_i + y_{ss} \sum_{i=1}^{m_p+m_f} g_i = k\frac{Y_{ss}}{L - x} - k\frac{y_{ss}}{L - x}$$

$$Y_{ss}\left[\sum_{i=1}^{m_p+m_f} f_i - \tfrac{k}{L-x}\right] = -y_{ss}\left[\sum_{i=1}^{m_p+m_f} g_i + \tfrac{k}{L-x}\right] \tag{30}$$

Since Y_{ss} and y_{ss} are arbitrary in value, each of the terms inside the brackets is equal to zero. This then leads to

$$\sum_{i=1}^{m_p+m_f} f_i = \tfrac{k}{L-x} \\ \sum_{i=1}^{m_p+m_f} g_i = -\tfrac{k}{L-x} = -\sum_{i=1}^{m_p+m_f} f_i \tag{31}$$

For the special case of $L = 1$, $x = L/2$ and $k = 1$, we obtain

$$\sum_{i=1}^{m_p+m_f} f_i = 2 \\ \sum_{i=1}^{m_p+m_f} g_i = -2 \tag{32}$$

Several observations can be made regarding the last two equations. First, they suggest a method of intrinsic verification [22] of the computations. That is, regardless of the value of the Tikhonov regularization parameter, the same sum should be obtained. Furthermore, the value must be very close to those given. Second, the sum for the g_i values is the negative of the sum for the f_i values. A consequence of this relation is that the temperature difference is the only important aspect; hence, the initial temperature is not needed, which is true for both steady-state and transient conditions. Also, both the temperatures can be in °C or K, for example.

Another type of insight from the filter coefficients can be obtained regarding the variances and standard deviations of the heat flux estimates. To obtain these estimates it is necessary to specify some statistical assumptions. Let the measurement errors be additive, have zero mean, have a constant variance σ^2 and be uncorrelated. Then the variance of Eq. (27) is

$$\sigma_q^2 = \mathbf{V}(\hat{\mathbf{q}}_\mathbf{M}) = \sum_{j=1}^{m_p+m_f} (\mathbf{f}_j^2 + \mathbf{g}_j^2)\sigma^2 \tag{33}$$

This result is independent of the subscript M. Some results are shown in Table 1 for three different locations $x_1/L = 0.25$, 0.5 and 0.75 and for three Tikhonov 1st order regularization parameters of $\alpha_T = 0.0001$, 0.001 and 0.01. The results in Table 1 are computed from Eq. (33) using an assumed measurement standard deviation of $\sigma = 1.0$. As shown in Table 1, as x_1/L increases, the standard deviation of the estimated heat flux increases. In contrast, they decrease as the regularization parameter increases.

6. Example

To illustrate the method to estimate the surface heat flux using a second subsurface sensor for the remote boundary condition, a finite domain of thickness $2L$ will be considered with a repeating triangular-in-time heat flux input at $x = 0$ and zero temperature at $x = 2L$. The variation can be seen in Fig. 8 (which also includes

Table 1
Standard deviations in the estimated heat flux for additive measurement errors with zero mean, constant variance σ^2, and uncorrelated. Results computed using Eq. (33) with $\sigma^2 = 1.0$. Columns 3 and 4 show the contributions σ_{q_Y} and σ_{q_y} of the measurements Y_i, and y_i on the total deviation σ_q shown in column 5.

$\frac{x_1}{L}$	α_T	σ_{q_Y}	σ_{q_y}	σ_q	$\sum_{j=1}^{m_p+m_f} f_j$	$\sum_{j=1}^{m_p+m_f} g_j$
0.25	0.0001	21.5939	4.7070	22.1010	1.3333	−1.3333
0.25	0.001	8.9798	2.7884	9.4028	1.3333	−1.3333
0.25	0.01	3.8136	1.5807	4.1282	1.3333	−1.3333
0.5	0.0001	25.4757	2.5751	25.6055	2.0000	−2.0000
0.5	0.001	10.1786	1.6262	10.3077	2.0000	−2.0000
0.5	0.01	4.2242	1.0085	4.3429	2.0000	−2.0000
0.75	0.0001	28.6552	1.9841	28.7238	4.0000	−4.0000
0.75	0.001	11.7680	1.5304	11.8671	3.9999	−4.0000
0.75	0.01	5.0194	1.1761	5.1554	4.0007	−3.9997

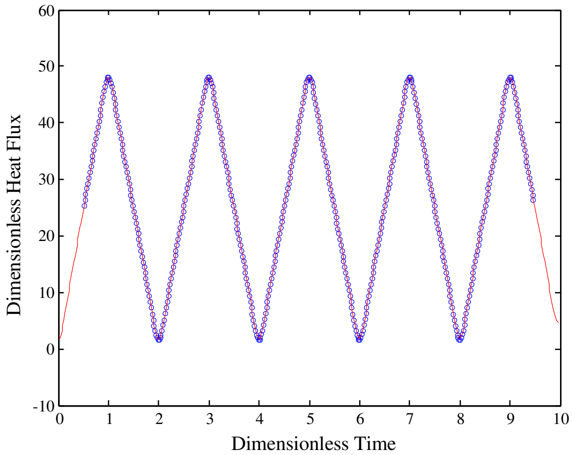

Fig. 8. Heat flux calculated using filter coefficients. Errorless data. Solid line is for Tikhonov whole domain, Circles are for the filter method. $x_1 = 0.5$; $L = 1$; $k = 1$; $\alpha = 1$; $T_L = 1$; $q_0 = 1$; $\Delta t = 0.02$; max = 500; $\alpha_{Tik} = 0.01$; (HTprofiles_2.m).

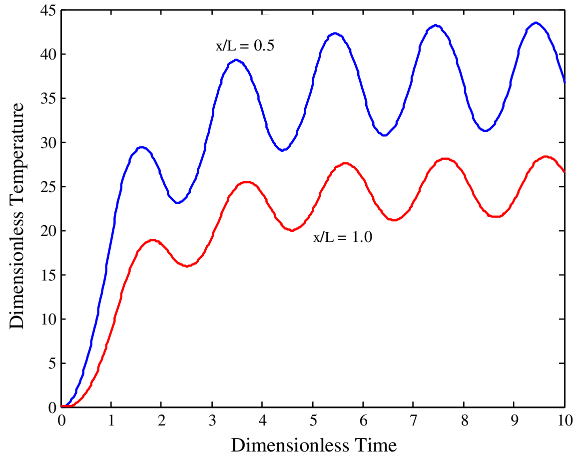

Fig. 9. Temperatures for several triangular heat flux components. $\Delta t = 0.02$; 50 time steps to get to peak. (HTprofiles_2.m).

results from the calculations, which will be explained below). Data for the remote temperature boundary is simulated from the solution at $x = L$ (that is, half-way through the domain of $2L$). "Measurements" are also extracted at $x_1 = L/2$ to simulate the sensor for the IHCP.

The temperatures at $x = L/2$ and L are shown in Fig. 9. The temperatures oscillate in an increasing damped manner and will eventually reach a quasi-steady state. The maximum temperature shown in Fig. 9 is about 43 in dimensionless temperature and the maximum surface temperature is about 50. These values are important to remember when introducing random errors; values small compared to these numbers are desired but should not be too small as to be unreasonable.

The IHCP problem is solved first with errorless data (to say, 10-digit accuracy). The temperature data illustrated by Fig. 9 at $x = L/2$ is for **Y** and the temperature at $x = L$ is for y. The whole domain Tikhonov method (Eq. (24)) and the sequential method based on filter coefficients coming from that method (Eq. (27)) are used and compared. The results for dimensionless time steps of 0.02 and $\alpha_T = 0.0001$ are shown in Fig. 8. Agreement between the Tikhonov whole-domain method and the filter analysis could hardly be better, it seems.

Note that, because of the width of the filter, values at the beginning and the end of the overall time range cannot be computed. The filter requires data from both past and future times, hence cannot be applied at the start, or at the finish. For this example, $m_p = m_f = 25$, so computations begin at the 26th time step and end 25 steps from the final time.

The filter method is best suited for an online application where results are computed continuously from a stream of data, such as in a continuous industrial process, and for such an application the start and stop intervals are not important. The result is a "near real-time" estimate of the time-varying heat flux, which is necessarily delayed by a relatively small number of time steps required to supply future data to the process. Considering the filter represented in Fig. 7, about 21 future times are required, based on the range of non-zero coefficients. The actual time delay depends on the thickness, L, and the thermal diffusivity, α. For a 1 cm thickness of carbon steel the delay is about 2.1 s, but for a 1 cm layer of organically-bonded glass fiber insulation the delay would be about 90 s.

Another case of interest is for relatively large simulated errors (additive, zero mean, constant variance, uncorrelated, and normally distributed). Normally distributed errors with a standard

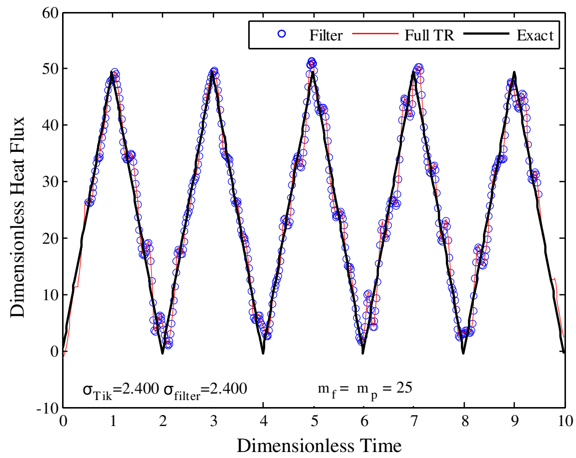

Fig. 10. Comparison of whole domain Tikhonov regularization with associated filter coefficient results for the case of "large" random errors ($\sigma_{error} = 0.5$, about 1% of maximum T). $x_1 = 0.5$; $L = 1$; $k = 1$; $\alpha = 1$; $T_L = 1$; $q_0 = 1$; $\Delta t = 0.02$; max = 500; $\alpha_{Tik} = 0.01$; (HTprofiles_2.m).

deviation of $\sigma = 0.5$ were added to the exact temperatures in Fig. 9, and these "noisy" data are processed using the two methods. The results are seen in Fig. 10 which uses $\alpha_T = 0.01$ and $m_p = m_f = 25$. Notice that the filter method gives the exact same results as the full TR method, and this is confirmed by the calculation of the standard deviation of the error between the recovered heat flux and the exact heat flux, which is equal 2.40 in both cases. The exact heat flux is shown as a heavy line in Fig. 10 for comparison.

Since the filter representation is really a manifestation of an underlying IHCP method (in this case, Tikhonov regularization), the performance of the filter with different heat fluxes will reflect the features of that particular solution method. Specifically, the degree of regularization afforded by the particular method will be retained. So, the degree of regularization chosen by the filter designer, which affects both bias and random error components in the solution [20], should be chosen with the type of heat flux (smoothly varying or rapidly-changing) anticipated in the target application.

The computer time to obtain results using the full Tikhonov regularization method is significantly more than that using the filter equation. Assuming that the filter coefficients are precomputed and stored, the computer time required using full TR method is approximately 25 times more than the required time for the filter method. About 500 simultaneous linear algebraic equations must be solved in the Tikhonov procedure for this example; one equation for every unknown heat flux component. The computation associated with the filter equation is trivial compared to this calculation. Furthermore, whole-domain direct solution time using Eq. (24) increases more than linearly with the number of unknown heat flux components. Also, computer memory requirements increase as more and more cycles are considered in a batch mode of analysis. That is not true for the filter computation. Thousands of cycles can be analyzed using the filter concept in an almost real-time fashion. It is only necessary to have a limited "window" of measurements available for temperatures at time t_M and a number of future and past temperatures relative to this time.

7. Conclusion

In this paper, a technique to account for the thermal action at a remote boundary in the IHCP solution using temperature data from a second sensor is outlined. Primary data needed for the solution is obtained from a sensor located at $x = x_1$, and supplemental data to account for the second boundary is measured at $x = L$, which may, or may not, correspond to a physical boundary. The IHCP solution is formulated into a filter representation. Using the filter technique, near real-time measurements can be continuously obtained, and this is suitable for industrial applications. The filter solution and a classical whole domain Tikhonov regularization solution are both applied to an example problem and the results match very well. The calculation time for the filter method is significantly smaller than the whole domain method which makes it an appropriate approach when real-time estimation of heat flux is required.

References

[1] J.V. Beck, B. Blackwell, C.R. St Clair Jr., Inverse Heat Conduction: Ill-Posed Problems, John Wiley and Sons, New York, 1985.

[2] O.M. Alifanov, Inverse Heat Transfer Problems, Springer-Verlag, Heidelberg, 1994.

[3] M.N. Ozisik, H.R.B. Orlande, Inverse Heat Transfer, Taylor & Francis, New York, 2000.

[4] D.A. Murio, The Mollification Method and the Numerical Solution of Ill-Posed Problems, John Wiley & Sons, New York, 1993.

[5] U. Ijaz, A. Khambampati, M.-C. Kim, S. Kim, K.-Y. Kim, Estimation of time dependent heat flux and measurement bias in two-dimensional inverse heat conduction problems, Int. J. Heat Mass Transfer 50 (2007) 4117–4130.

[6] H.-T. Chen, S.-Y. Lin, L.-C. Fang, Estimation of surface temperature in two-dimensional inverse heat conduction problems, Int. J. Heat Mass Transfer 44 (2001) 1455–1463.

[7] J.M. Mulcahy, D.J. Browne, K.T. Stanton, F.R.C. Diaz, L.D. Cassady, D.F. Berisford, R.D. Bengtson, Heat flux estimation of a plasma rocket helicon source by solution of the inverse heat conduction problem, Int. J. Heat Mass Transfer 52 (2009) 2343–2357.

[8] W.-L. Chan, Estimation of heat flux on the surface of an initially hot cylinder colled by a laminar confined impinging jet, Int. J. Heat Mass Transfer 55 (2012) 597–606.

[9] S. Khajehpour, M.R. Henatiyan, L. Marin, A domain decomposition method for the stable analysis of inverse nonlinear transient heat conduction problems, Int. J. Heat Mass Transfer 58 (2013) 125–134.

[10] T. Chen, S. Lin, J.C.Y. Wang, Determination of the boundary temperature errors by variation of two temperature sensor locations in a one-dimensional inverse heat conduction problem, Int. J. Numer. Meth. Heat Fluid Flow 7 (7) (1997) 635–646.

[11] A.N. Tikhonov, Regularization of incorrectly posed problems, Soviet Math. 4 (1963) 1624–1627.

[12] A.N. Tikhonov, On the Solution of Incorrectly Formulated Problems and the Regularization Method 4 (1963) 1035–1038.

[13] M. Khorrami, F. Samadi, F. Kowsary, M. Mohammadzaheri, Online estimation of multicomponent heat flux using a system identification technique, Internation Communications in Heat and Mass Transfer, 44 (2103) 127-134.

[14] S. Deng, Y. Hwang, Applying neural networks to the solution of forward and inverse heat conduction problems, Int. J. Heat Mass Transfer 49 (2006) 4732–4750.

[15] M. LeBreux, M. Delilets, M. Lacroix, Fast inverse prediction of phase change banks in high temperature furnaces with a Kalman filter coupled with a recursive least-square estimator, Int. J. Heat Mass Transfer 53 (2010) 5250–5260.

[16] P.K. Lamm, Z. Dai, On local regularization methods for linear Volterra equations and nonlinear equations of Hammerstein type, Inverse Prob. 21 (2005) 1773–1790.

[17] P.K. Lamm, Full convergence of sequential local regularization methods for Volterra inverse problems, Inverse Prob. 21 (2005) 785–803.

[18] J.M.G. Cabeza, J.A.M. Garcia, A.C. Rodriguez, Filter digital form of two future temperature methods for the inverse heat conduction: A spectral comparison, Int. J. Numer. Methods Biomed. Eng. 26 (2010) 554–573.

[19] J.M. Gutierrez, J.A. Martin, A. Corz, A sequential algorithm of inverse heat conduction problems using singular value decomposition, Int. J. Therm. Sci. 44 (2005) 235–244.

[20] K.A. Woodbury, J.V. Beck, Estimation metrics and optimal regularization in a Tikhonov digital filter for the inverse heat conduction problem, International Journal of Heat and Mass Transfer 62 (2013) 31–39.

[21] J.V. Beck, Filter solutions for the nonlinear inverse heat conduction problem, Inverse Problems in Science and Engineering 16 (1) (2008) 3–20.

[22] K.D. Cole, J.V. Beck, A. Haji-Sheikh, B. Litkouhi, Heat Conduction Using Green's Functions, 2nd Ed., CRC Press, 2011.

[23] J.V. Beck, N.T. Wright, A. Haji-Sheikh, Transient power variation in surface conditions in heat conduction for plates, International Journal of Heat and Mass Transfer 51 (2008) 2553–2565.

[24] K. Cole, EXACT Number Tutorial, in *ExACT* Analytical Conduction Toolbox , retrieved August 2013, from http://exact.unl.edu/exact/home/number.php.

[25] A. N. Tikhonov, V. Y. Arsenin, Solutions of Ill-posed Problems, Washington, DC: V. H. Winston & Sons, 1977.